CHAPTER 4

GAMMA - HADRON DISCRIMINATION

4.1 INTRODUCTION

High-energy γ-ray astronomy provides a very valuable source of information regarding non-thermal processes in the Universe. In recent years this field has progressed significantly. The γ-ray sky at energies over 10 TeV is also of the astrophysical importance since it can give essential clues regarding the origin of galactic CRs of very high energy. The *ultra-high energy* (UHE) CRs arriving at the Earth are mainly charged particles and a small fraction of γ-rays. In their travel through the interstellar medium, charged particles have their paths affected by electromagnetic fields and interstellar gas clouds, although γ-rays arrive directly from their sources, giving information about the physical processes which take place at/near their source engines. Also the heliosphere and interplanetary medium interact with charged particles, while γ-rays retain their original information about sources. When CRs arrive at the top of the atmosphere they generate EASs that develop through the atmosphere until they reach ground level. The EAS thus formed can be detected by observing (**a**) the secondary particles arriving on the ground; (**b**) Cherenkov light emitted by charged secondary particles and (**c**) fluorescence light emitted by charged secondary particles. These particle signals are observed by means of different experimental techniques.

The EGRET telescope aboard the Compton Gamma-ray Observatory (Collmar 2000) has detected over two hundred point sources. A significant number of these sources emit γ-rays with energy up to a few GeV. This upper limit is due to the restricted collection area of satellite-based observatories. Since for many of these sources no spectral cuts have been observed, they are expected to emit γ-rays at higher energies. These promising results have promoted the design of advanced ground based telescopes which detect the secondary particles of the shower. The most successful ground based devices are the so-called *imaging air-Cherenkov telescopes* (IACTs) (Aharonian 2006[a]). The IACTs such as MAGIC (Baixeras et al. 2003 & MAGIC Coll. 2008), H.E.S.S. (Hinton 2004), VERITAS (Weeks 2010 & Beillicke 2008) and the onboard Fermi Large area telescopes (FermiLAT) (Atwood 2009 & Dermer 2012) produce results which agree remarkably well with

the astrophysical model predictions. Observations by FermiLAT revealed more than 1,873 high-energy gamma-ray sources, including several classes of active galaxies, pulsars, pulsar wind nebulae, supernova remnants, binary sources, high-energy gamma-ray bursts, a nova and the Sun (Michelson 2011). The imaging technique provides a method of effectively discriminating between γ-rays initiated showers and the background CR showers, based on the morphology of their Cherenkov images. Careful analysis of anomalies in the structure of EASs is the only possible way to obtain experimental information about UHE γ-rays in primary cosmic radiation and provides the means to study CRs beyond the flux limits of direct observations (energies larger than 10^{14} eV). From the literature study it is known that the EAS observables like shower size (N_e), muon size (N_μ), hadron size (N_h), air shower associated Cherenkov content (N_{Ch}), and morphology of the Cherenkov images and the depth of shower maximum (X_{max}) were generally used for the purpose of gamma-hadron discrimination from time to time. To extract information about primary CRs more accurately from the experimental measurements, detailed MC simulations of the shower development is being used as basis of the data analysis and interpretation. The MC simulations consider the evolution of EAS in the atmosphere initiated by different energetic particles which propagates down to observation level.

In the field of CR air shower physics, the separation of γ-rays from the dominant nuclear component in the cosmic radiation is an important topic for astroparticle physics that still needs more attention (Nestnhoff et al. 1995 & Badran et al. 1997). The UHE γ-rays are considered to be an hadronic origin of primary CRs: a fraction of accelerated hadronic CRs are likely to produce γ-rays through Δ-resonances, bremsstrahlung, inverse Compton etc. non-thermal processes at or very close to the source site by interacting with the ambient matter (Bhadra & Dey 2009). The γ-ray detection suffers from the huge background constituted by ordinary (nucleonic) CRs in the GeV-TeV energy region. The flux of primary γ-rays amongst the CRs has been estimated to be $\sim 10^{-5}$ of the proton flux at 100 TeV (Wolfendale 1990). However, some early works predicted a galactic plane excess higher than this: $\frac{\gamma}{p} \sim 10^{-2}$, 3×10^{-2} and 10^{-2} at 10^2, 10^3 and 10^4 TeV (Wdowczyk et al. 1983). Even at energy of 10^7 TeV, this ratio has been predicted to rise up to 10^{-1}(Wdowczyk et al. 1983). To observe astrophysical sources (emitting undeflected γ-rays and assumed as point-like objects) and to

study the anisotropy properties of primary CRs, one has to eliminate isotropically distributed CRs.

Hadronic showers produce muons in the charged pions and kaons decays that occur in the hadronic interactions, while showers initiated by γ-rays/$e^{\pm}$ are purely electromagnetic except for hadrons photo-production, that is, a hadronic interaction of a photon with an air nucleus. The photo-production cross section increases with primary energy and consequent upon, γ-ray initiated air showers would have a significantly less muon content than those of hadronic cascades at low energy (Gaisser 1990 & Gandhi et al. 1990). Usually poor muon content is considered as the signature of γ-ray initiated EAS. In order to select a γ-ray shower based on such a criterion, an EAS array needs to be equipped with muon detectors covering very large area which is economically very challenging and such a facility is rarely available. So one has to look for some other primary mass sensitive observables based on which γ-ray initiated EASs can be separated out without the need of large area muon detector. In some early works, efforts were made to distinguish γ-ray showers on the basis of developmental stage of EAS in the atmosphere with the idea that γ-ray induced EAS will be younger than the hadron initiated EAS (Samorski et al. 1983 & Protheroe et al. 1984). The lateral shower age ($s_{\perp}$) is essentially the slope of the lateral density distributions of electrons in EAS that reflects the developmental stage of EAS and hence $s_{\perp}$was used as distinguishing parameter (Greisen 1956, Greisen 1960 & Snyder 1989). However, earlier MC simulation results regarding youthfulness of γ-ray showers in terms of shower age were inconclusive (Fenyves 1985 & Hillas 1987). In those simulation works, authors used their own simulation codes and findings could not be cross checked. Since, nowadays standard simulation code like CORSIKA (Cosmic Ray Simulation for KAscade) (Heck et al. 1998 & Capdevielle 1992) is available and our knowledge about the high energy particle interactions is much improved now, it would be imperative to revisit the issue.

4.2 METHODS FOR SELECTING GAMMA-RAY INDUCED SHOWERS

In this chapter, we have presented a detailed study on discrimination of γ-ray induced EAS from the background contributed by hadrons in the multi-TeV range. The lateral shower profiles generated by various primaries within a particular primary energy range are being used here, and they provide some discriminatory power for separating γ-ray showers from the background. The

selection of γ-ray showers is attempted by employing two different approaches – the **Method I** and the **Method II**. In the former approach (Method I), we have taken single (r-independent) lateral age parameter i.e. $s_{\perp}$ as the γ-ray separation parameter. Besides, it has been argued in the literature that the different masses of primary CRs might also be separated out by the simultaneous use of N_e, N_{μ} and f parameters (Sciascio et al. 2007 & Aloisio et al. 2001). The parameter f is giving out the ratio of reconstructed average electron densities at two arbitrary distance bands from the shower core, measuring roughly the rate of absorption of electrons in their lateral developments from the shower core. Experimentally it is observed that the NKG function with a single lateral age is insufficient to describe the lateral density distribution of EAS electrons properly at all distances, which implies that the lateral age changes with the radial distance. Subsequently, the notion of local lateral shower age parameter (LAP) was introduced (Capdevielle & Gawin 1982, Bourdeau et al. 1980 & Capdevielle et al. 1990) which is in essence the lateral age at a point. A detailed description of the LAP has already been outlined in the **chapter 3**. Since experimental electron density data in EAS may fluctuate considerably at a particular radial distance, instead of taking LAP at any particular point we take an average LAP nearly between 50 m and 300 m. In Method II we employed this average LAP (s_{local}) to select γ-ray showers. It is found that when single constant age ($s_{\perp}$) is used, the separation power becomes subdued. In contrast, the average LAP appears as a suitable mass sensitive parameter for classifying γ-ray induced showers.

4.3 OBSERVATIONAL LEVELS OF INTEREST

The present study has been performed mainly at the geographical location of ARGO-YBJ (latitude 30.11^0 N, longitude 90.53^0 E, 4300 m a.s.l.) (Sciascio 2007 & Aloisio 2001). This is because the experiment offers a full coverage array and hence can measure radial density distribution of electrons in EAS with great accuracy, which in turn provides an opportunity to estimate LAP accurately. Moreover, since ARGO-YBJ does not have any muon detector, discrimination of γ-ray showers based on an alternative EAS observable, related to only electromagnetic component should be very useful. The proposed observable may be of interest for surface detectors (SD) experiments, that have no any (or reliable) measurements of the muonic shower size. Since ARGO-YBJ experiment is located at very high altitude, its energy threshold is sub TeV and hence for this location we

simulated EAS events in the energy range from 1 TeV to 3 PeV. However, ARGO-YBJ has not yet studied the radial variation of the lateral shower age while a few other experiments, such as Akeno (Nagano et al. 1984[a] & Nagano et al. 1984[b]) and NBU (Sanyal et al. 1993), successfully tested the predicted radial variation of LAP. We simulated a few events at the geographical location of Akeno and compared with the observations to demonstrate again the importance of considering LAP instead of single shower age. The correlations of $s_{\perp}$ with N_e and/or N_{μ} have been considered as a basis for extracting information on the nature of primary CRs. The KASCADE (Antoni et al. 2001) and the NBU (Bhadra et al. 1998) experiments provide a few results on these aspects. Accordingly we performed simulations at the geographical locations of these experiments and compared with experimental findings in order to examine primary mass sensitivity of lateral shower age parameter.

4.4 SIMULATION CHARACTERISTICS

The MC simulation for generating EAS events considers interaction mechanisms of energetic particles as input. But due to limited knowledge of particle interactions at high energies (and the large fluctuations) the results of simulation may become model dependent. To ensure that the conclusion of the present work is robust, we consider two high energy hadronic interaction models, QGSJet **01** v.**1c** (Kalmykov et al. 1997) and EPOS **1.99** (Werner et al. 2006 & Pierog & Werner 2008[a]) and found that the present findings do not have any strong dependence on the choice of interaction model.

The EAS events are simulated by coupling the high energy hadronic interaction models mentioned in the previous sentence, and the low energy hadronic interaction model GHEISHA (version **2002d**) (Fesefeldt 1985) in the framework of the CORSIKA MC program version **6.970** (Heck et al. 1998 & Capdevielle 1992). For the electromagnetic part the EGS4 (Nelson et al. 1985) program library has been used. The maximum zenith angle of primaries has been restricted to 45 degree here.

The MC simulation data library consists of over 0.1 million EAS events each for p, Fe and γ-ray at the ARGO-YBJ location in the primary energy range 1 TeV to 3 PeV using both QGSJet **01** and EPOS **1.99** models. In addition, we have generated 25,000 EAS events for each primary component p, Fe and γ-ray and

about 10,000 He events with the model QGSJet in the primary energy range from 100 TeV to 30 PeV following a power law with a spectral index of -2.7 below the *knee* and -3.0 above the *knee* at the geographical locations of KASCADE (latitude 49.1^0 N, longitude 8.4^0 E, 110 m a.s.l.) and NBU (latitude 26.8^0 N, longitude 88.4^0 E, ~130 m a.s.l.). Besides, a small size of EAS events for p and Fe primaries are generated at the location of Akeno (latitude 35.78^0 N, longitude 138.5^0 E, 900 m a.s.l.). The magnetic fields are set for all four observational levels accordingly.

Two mixed compositions have been prepared from the generated showers taking 50% p, 25% He, 25% Fe events forming **mixture-I** and 37% p, 37% Fe, 26% γ-ray events constituting **mixture-II** respectively for better understanding of EAS observational results.

4.5 THEORETICAL BACKGROUND AND SIGNAL SELECTION TECHNIQUE

4.5.1 THE LATERAL AND LOCAL AGE PARAMETERS

Extensive air showers propagating in the same density profile of the atmosphere essentially have equal lateral distributions around the shower axis. In the cascade theory, the problem of deriving the electron lateral distribution through an analytical method received an important recognition in the past. Nishimura and Kamata (Lipari 2009) solved numerically the 3-dimensional shower equations in *Approximation B* to obtain the lateral distribution of electrons propagating in a medium of constant density. The results obtained on lateral density distribution of cascade particles by Nishimura and Kamata can be approximated by the well known Nishimura-Kamata-Greisen (NKG) structure function proposed by Greisen (Greisen 1956, Greisen 1960 & Snyder 1989) that has been written through the *equation* (**3.4**) in **Chapter 3**. Using that equation, the electron density can be given by:

$$\rho(r, s_\perp) = N_e C(s_\perp)(\frac{r}{r_m})^{s_\perp - 2}(1 + \frac{r}{r_m})^{s_\perp - 4.5}, \qquad (4.1)$$

The symbols have their usual meaning as discussed in the preceding chapter. But such a widely used relation in (**4.1**) does not hold if $s_\perp$ varies with r, as noted in Akeno (Nagano et al. 1984[a] & 1984[b]), NBU (Sanyal et al. 1993) and some other observations (Capdevielle & Gawin 1982, Bourdeau et al. 1980 & Capdevielle et al. 1990). An improvement of the NKG function was proposed by adopting a modulated, longitudinal age parameter $s_\parallel / s_L$ dependent effective Moliere radius

(Lagutin et al. 1979 & Uchaikin 1979) by the relation (**3.6**) but the lateral shower age is still found to vary with radial distance experimentally. To tackle the situation a method was developed by Capdevielle *et al* introducing the concept of *local age parameter* (LAP) (Capdevielle & Gawin 1982, Bourdeau et al. 1980 & Capdevielle et al. 1990). The formula for the LAP estimated in a small radial distance band $\{x_i, x_j\}$ from the shower core is given by the following relation.

$$s_{local}(i,j) = \frac{\ln\left(F_{ij}X_{ij}^{2}Y_{ij}^{4.5}\right)}{\ln\left(X_{ij}Y_{ij}\right)} \qquad (4.2)$$

The different notations used in the above equation (**4.2**) have been pointed out previously in the equation (**3.7**). The identification $s_{local}(r) \equiv s_{local}(i,j)$ for $r = \frac{r_i + r_j}{2}$ remains valid for the experimental distributions as far as they are approximated by monotonic decreasing functions versus radial distance (note that, $s_{local}(r) \equiv s_{local}(i,j) \equiv s_{\perp}^{local}(r) \equiv s_{ij}^{local}$).

In the present work, we have given emphasis on the estimation of the LAP and on its average using $s_{local}(r)$ values, taken between first minimum and the subsequent maximum from the radial variation of LAP. The estimation of $s_{\perp}$ would also be made through the traditional shower reconstruction method.

4.5.2 BACKGROUND REJECTION: THE QUALITY FACTOR

In the present work the LAP has been proposed to separate γ-ray showers from hadronic ones. In order to understand how LAP and $N_e$work together to optimise their functioning, the general expression for the γ-*ray*-to-background (likewise signal-to-noise ratio is used for detectors performance) shower ratio as a linear function of a parameter Q:

$$\frac{signal}{noise} \equiv \frac{desired\ events}{undesired\ events} \propto Q(E, N_e, s_{local}, \theta) \qquad (4.3)$$

where Q is the γ-ray or hadron identification efficiency and is known as the quality factor. The background rejection or γ-ray acceptance is usually made by numerical maximization of the parameter Q within an appropriate zenith angle, primary energy and N_e ranges corresponding to appropriate cut applied on s_{local}. The quality factor Q essentially quantifies the gain of significance of the applied cut achieved by the separation algorithm. It is defined as

$$Q = \frac{\epsilon_\gamma}{\sqrt{\epsilon_{bkg}}} = \frac{\epsilon_\gamma}{\sqrt{(1-\xi_{bkg})}} \qquad (4.4)$$

, where ϵ_γ and ϵ_{bkg} are respectively the γ-ray and background acceptances from the sample using a cut value of s_{local} while ξ_{bkg} stands for the rejection of background. Here, $\epsilon_\gamma = \frac{n_{\gamma(cut)}}{n_\gamma}$ and $\epsilon_{bkg} = \frac{n_{bkg(cut)}}{n_{bkg}}$, with $n_{\gamma(cut)}$ and $n_{bkg(cut)}$ represent number of showers of either kind passing a particular cut value of s_{local} whereas n_γ and n_{bkg} are the number of all triggered events (before cuts).

The significance of the selection enhancement can also be evaluated with the so-called sensitivity parameter as well and it is defined by the following,

$$S = \frac{n_{\gamma(cut)}}{\sqrt{n_{bkg(cut)}}} \qquad (4.5)$$

where the denominator is the fluctuation of the background showers which actually measures the hadron contamination present in the selected γ-ray (signal) showers.

4.6 ESTIMATION OF SHOWER AGE PARAMETERS

The simulated electron density data have been analyzed in two different methods to obtain shower age parameters $s_\perp$ and $s_{local}(r)$. First, following the traditional approach we estimate $s_\perp$ (along with other shower parameters) by fitting the density data with the NKG structure function using our own reconstruction algorithm. In this approach, the simulated electron densities at different radial distances have been fitted by the method of chi-square minimization through an iterative procedure based on the method of steepest decent to the NKG lateral distribution function of electrons. Here it is to be noted that majority of the EAS groups generally estimate basic shower parameters based on the NKG function. In order to check the goodness of the NKG function in describing the simulated radial density distribution of electrons, we firstly fitted the simulated density data at various radial distances with the NKG function and compared radial density distribution of electrons for simulated events with the fitted curve. Fitted showers with reduced χ^2 less than 5 are only accepted for results involving $s_\perp$. The error in estimating $s_\perp$ in the N_e range $1.5 \times 10^4 - 4.25 \times 10^5$ has been found as ± 0.03.

We directly estimated LAP for each individual shower exploiting equation (4.2). We noted that the description of the data by the NKG function is improved when the Moliere radius is treated as a variable rather than a fixed parameter (Dey

et al. 2012). But this description comes at the expense of very high shower age value which somewhat obscures the physical meaning of the age parameter as assigned in the cascade theory. In this analysis, the error of the LAP for EAS with the primary energy in the PeV range remains within 0.05 for $10m < r < 250m$, whereas for $r < 10m$ or when $r > 300m$ the error of the LAP is found to be higher, about 0.1.

It has shown recently (Dey et al. 2012) that LAP initially decreases with radial distance, reaches a minimum around 50 m, then starts increasing with radial distance, attains a local maximum around 300 m and decreases again thereafter. The nature of such a variation of LAP with radial distance was found independent of energy of the shower initiating particles (Dey et al. 2012). We observed such a characteristic variation of LAP with radial distance at ARGO-YBJ location as shown in **Fig.4.1a** for protons, irons and γ-rays. It is seen from the figure that the nature of variation is nearly the same for both QGSJet and EPOS. Here, it is worthwhile to main that up to 50 TeV or so, the density of electrons in EAS beyond 50 m from the shower core is extremely small even at ARGO-YBJ level and is almost impossible to measure it in practical situation. Hence, we have chosen primary energy from 100 TeV and above for results.

As already mentioned, Akeno group studied the radial variation of LAP (Nagano et al. 1984[a] & Nagano et al. 1984[b]). We compared our simulation results with Akeno observations in **Fig.4.1b** for proton and iron primaries. The single lateral shower age $s_{\perp}$for proton and iron are also given (solid and dashed lines parallel to the x-axis) in the figure for comparison. We also estimated LAP from the lateral density distribution of electrons obtained by the KASCADE experiment (Antoni et al. 2001, Apel et al. 2006 & Ulrich et al. 2008 & 2009[a]) and we compared with our simulation results in **Fig.4.1c**. The errors in the extracted experimental points are quite large but it is at least clear that a constant single lateral shower age is insufficient to describe the experimental findings.

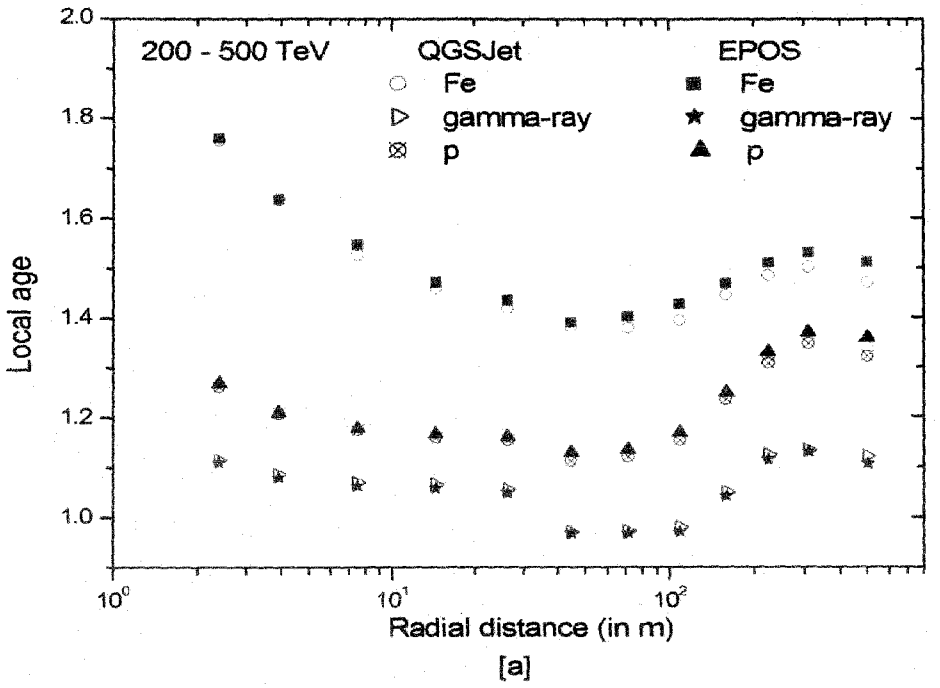
200 - 500 TeV
QGSJet
Fe
gamma-ray
p
EPOS
Fe
gamma-ray
p
Local age
Radial distance (in m)

[a]

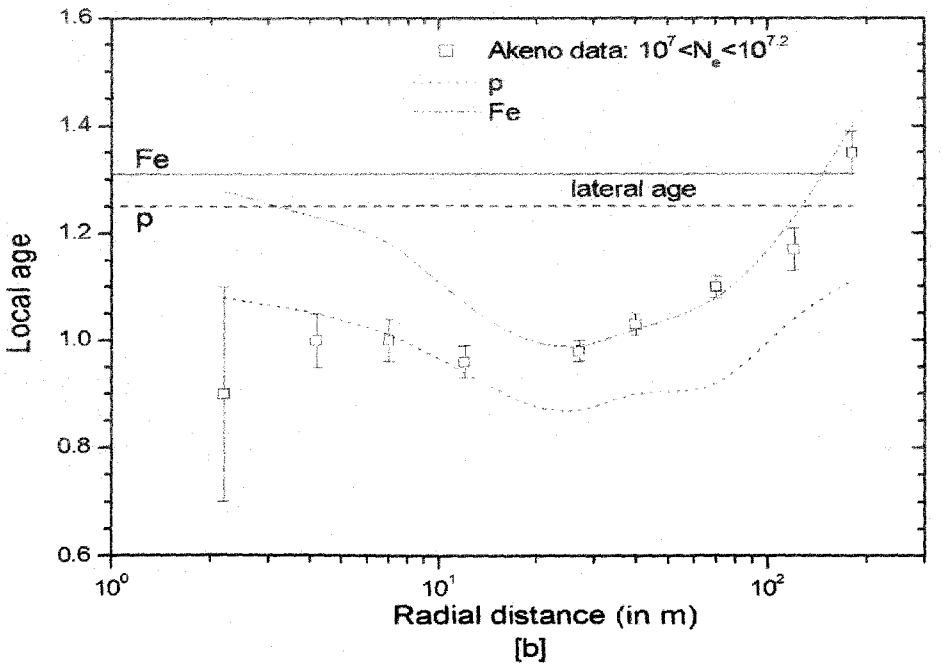
Akeno data: $10^7 < N_e < 10^{7.2}$
p
Fe
Fe
lateral age
p
Local age
Radial distance (in m)

[b]

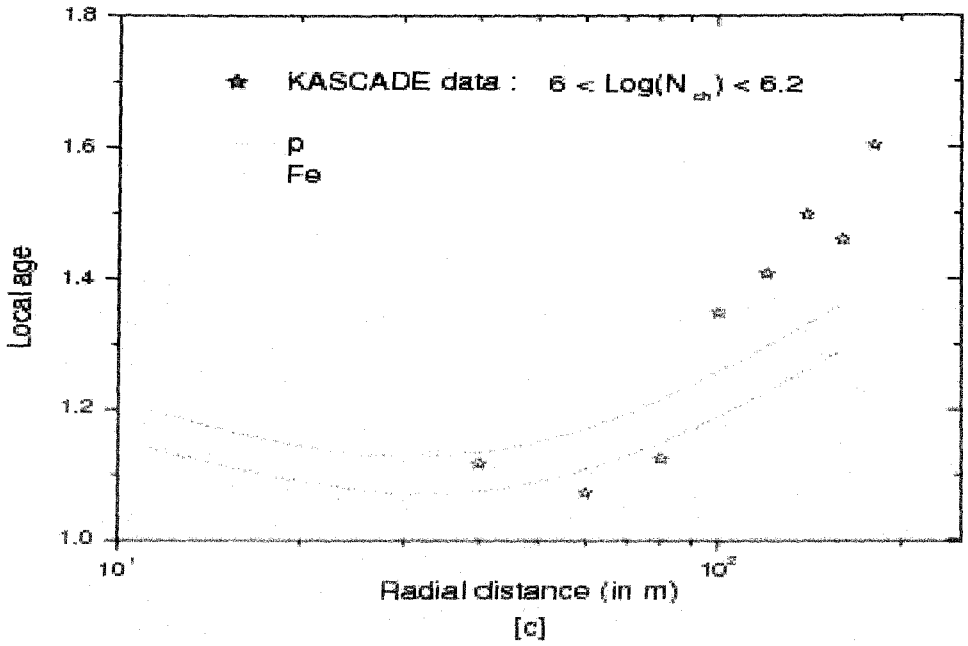

Fig.4.1: [a] The radial variation of LAP obtained at the ARGO-YBJ altitude for p, Fe and γ-ray with hadronic interaction models QGSJet and EPOS. [b] Same as Fig.4.1a at the Akeno level with QGSJet model, compared with experimental data. The solid and dashed lines parallel to the x-axis indicate $s_{\perp}$ for Fe and p. [c] The radial variation of LAP estimated from the KASCADE observed lateral distribution data. Lines indicate the mean values of a sample of simulated EAS events with QGSJet model (the errors in experimental data are not included here).

Since air shower measurements are subjected to large fluctuations, instead of LAP at a particular radial distance we consider for each event a mean LAP ($< s_{local} >$), which is the average of all LAPs for various distance bands (r_i, r_j) over the radial distance taken from 50 m to 300 m. For the purpose of averaging, distance bands are taken in constant steps on the logarithmic scale. The radial distance band from 50 m to 300 m is chosen because the positions of local minimum and maximum at 50 m and 300 m are nearly universal, independently of primary energy and species (Dey et al. 2012).

4.7 RESULTS ON GAMMA-HADRON SEPARATION: METHOD I

The simulated EAS events so generated have been analyzed by employing **method I** at NBU and KASCADE locations (both at sea level) to investigate some important distinguishing features of γ-ray and hadron induced air showers. The observable parameters like $s_{\perp}$, N_e, N_{μ} and N_h are being used. Results obtained

from these studies have been compared with some of the published results of NBU (Bhadra 1999) and KASCADE (Antoni et al. 2001) respectively. In this section, the gamma-hadron separation has also been performed with the help of local electron densities (i.e. ρ_1 and ρ_2), N_e and N_μ at the ARGO-YBJ location.

4.7.1 N_e AND N_μ DEPENDENCIES OF $< s_\perp >$

The correlation between the mean lateral shower age $< s_\perp >$ over a small shower size bin in the range $10^3 - 1.5 \times 10^6$, with the zenith angle interval $0^0 - 45^0$ for p, Fe, γ-ray and mixed composition (mixture-I) using QGSJet model and corresponding NBU results (Bhadra 1999) are put on view in **Fig.4.2a**. The NBU EAS experiment reported the total uncertainties (including instrumental uncertainty) in estimating $s_\perp$ and $N_e$as $\pm 9\%$ and $\pm 0.14 N_e$ (Bhadra et al. 1998). It is important to perceive that the lateral shower age takes higher values for heavy nuclei compared to that of light and γ-ray primaries clearly indicating relatively flatter lateral distribution of electrons as one move from γ-ray to Fe via p.

The variation of $< s_\perp >$ with muon size in the primary energy range $10^2 - 3 \times 10^4$ TeV and zenith angle interval $0^0 - 45^0$ for p, Fe, γ-ray primaries is presented in **Fig.4.2b** with KASCADE experiment using NKG fitting for muons with slightly higher muon threshold energy. The **Fig.4.2b** exhibits the fact that γ-ray initiated showers can be separated out from the background using $< s_\perp >$ and N_μ. It was also concluded in one of our previous work that EASs due to light primary components are younger on the average (Dey et al. 2012).

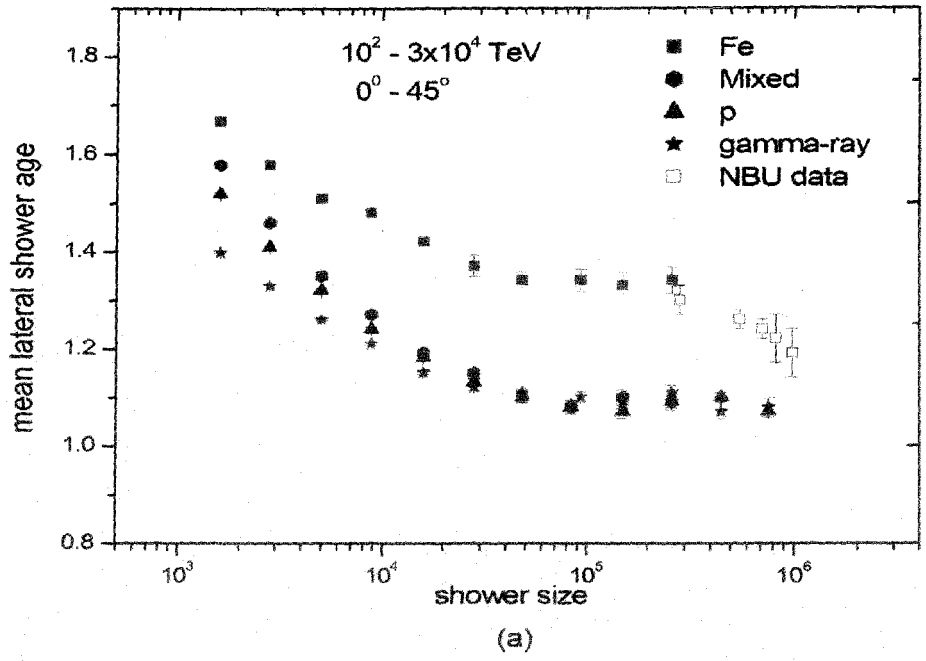

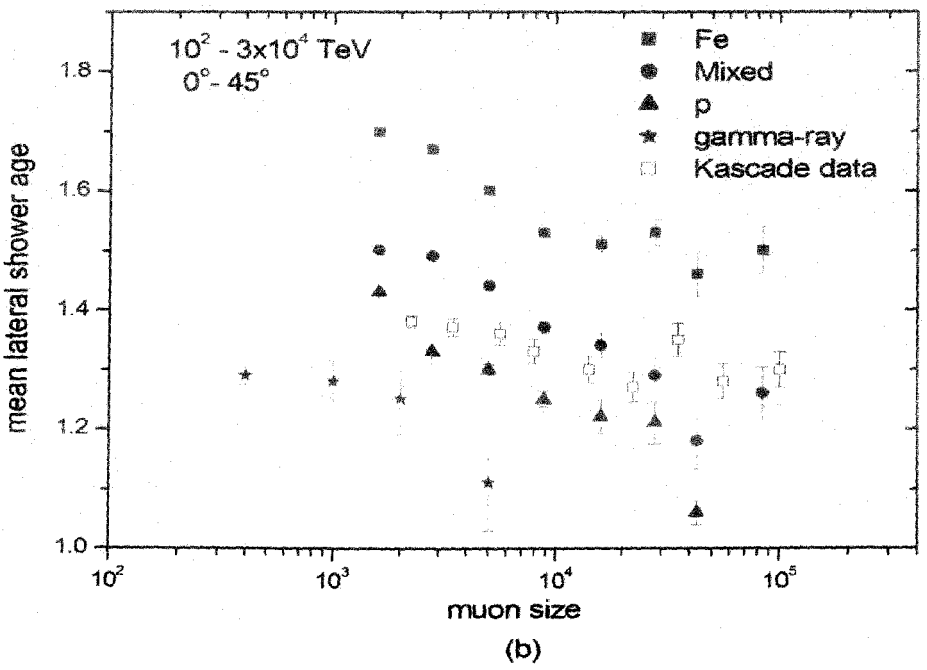

Fig.4.2: [a] Variation of mean lateral shower age with shower size along with NBU data; [b] Variation of mean lateral shower age with muon size. For comparison with KASCADE data in Fig.4.2b, where the age parameter was estimated by NKG fits with r_μ as 420 m and also used truncated muon sizes N_μ^{tr}. The QGSJet model has been used for simulation.

The KASCADE data points indicate that the composition changes slowly from predominantly proton at around 10^{14} eV to heavier primaries with the increase of energy. The NBU data are available only over a small energy window and though both the NBU and the KASCADE data suggest for a mixed composition in the common energy range of study, the NBU data favour for a relatively heavier composition. However, being a small EAS array the NBU experiment could measure electron density only up to 80 m from the shower core and its resolution power for primary composition is thus limited.

4.7.2 VARIATION OF f WITH g

The lateral structure of EAS from different primaries attributes some power of identification and rejection hadron primaries from γ-ray with the same primary energy and size (Sciascio et al. 2005). From the lateral profile of each simulated EAS event, we have estimated electron densities at five adjacent radial points in each of the two arbitrarily chosen distance bands $5-15$ m and $35-45$ m. Next by employing the reconstruction procedure for the determination of local electron density (LED), we obtained two average reconstructed LEDs $\rho_1$and ρ_2 from the shower core.

The selection of γ-ray showers from hadrons becomes visible when one plots the parameter f against g where $g \equiv \frac{N_\mu}{N_e}$ as presented in a $2-$dimensional **Fig.4.3a** using the high-energy interaction model QGSJet. The same study has been repeated for another pair of radial bands $20-30$ m and $50-60$ m, using the same sample of mixture-II and it is depicted in **Fig.4.3b**. The rate of absorption of electrons decreases with increasing radial distance from the core and this feature is revealed from the comparison of **Fig.4.3a** and **Fig.4.3b**. We have checked through the **Fig.4.3c** that the characteristic feature of the $g-f$ distribution does not change appreciably for the high energy interaction model EPOS. Even for a different primary energy range such as 100 - 200 TeV we have found the similar behaviour in $f$against$g$.

It appears from **Figs. 4.3** that this technique essentially exploits the total muon content in an EAS. The EAS events are classified according to their primaries along x-axis (the ratio of muon size to electron size is plotted along x-axis); there is no notable separation along y-axis between events generated by photons and protons.

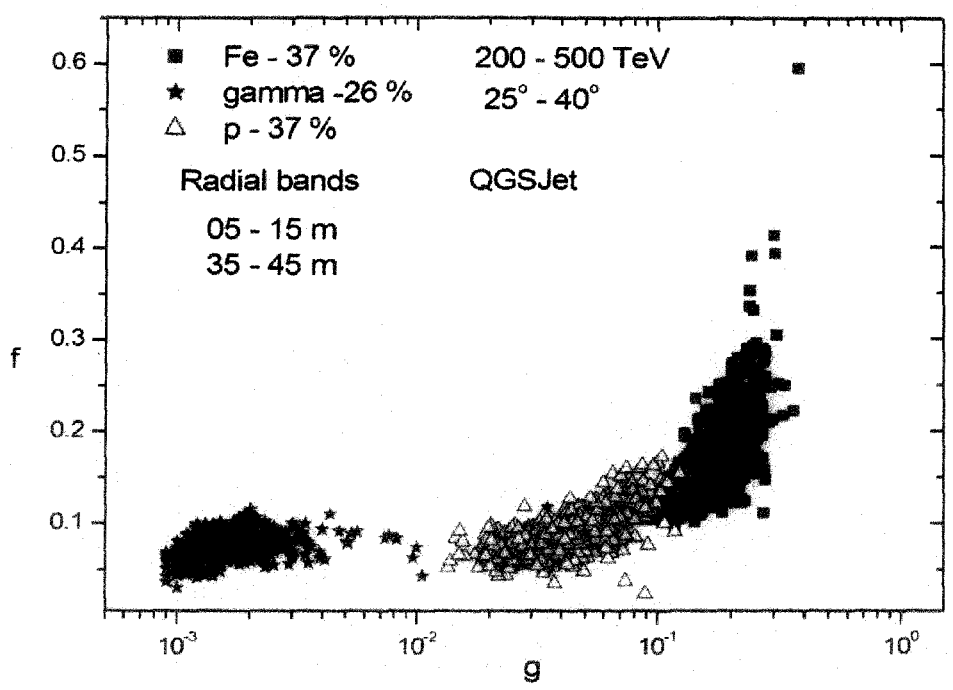
Fe - 37 %
gamma -26 %
p - 37 %
200 - 500 TeV
25° - 40°
Radial bands
QGSJet
05 - 15 m
35 - 45 m
f
g
0.6
0.5
0.4
0.3
0.2
0.1
10^-3
10^-2
10^-1
10^0

[a]

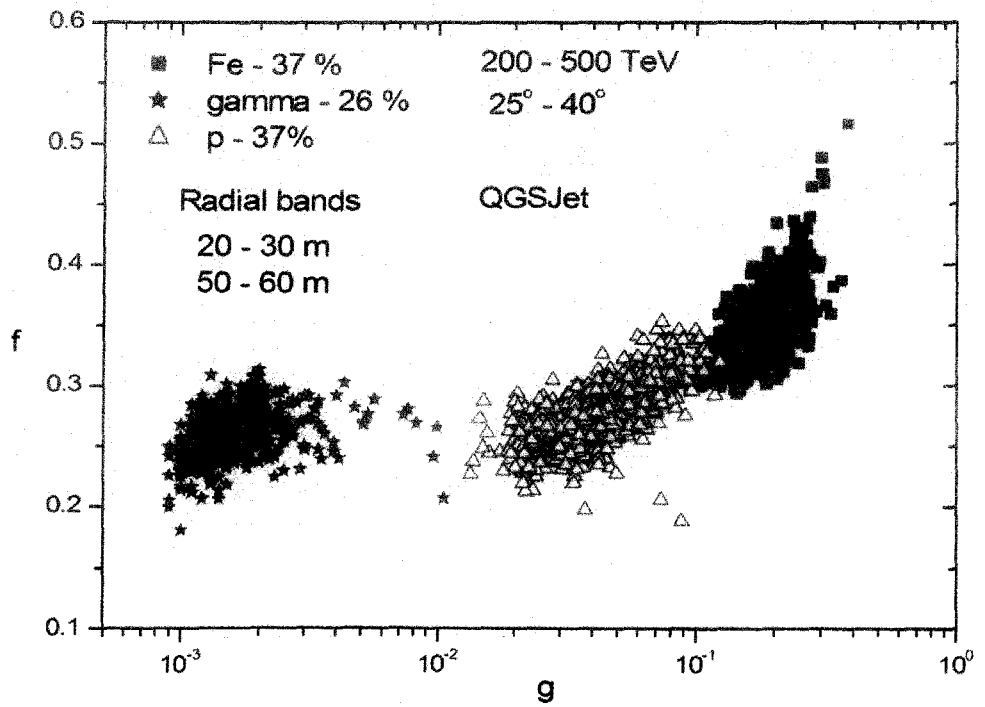
Fe - 37 %
gamma - 26 %
p - 37%
200 - 500 TeV
25° - 40°
Radial bands
QGSJet
20 - 30 m
50 - 60 m
f
g
0.6
0.5
0.4
0.3
0.2
0.1
10^-3
10^-2
10^-1
10^0

[b]

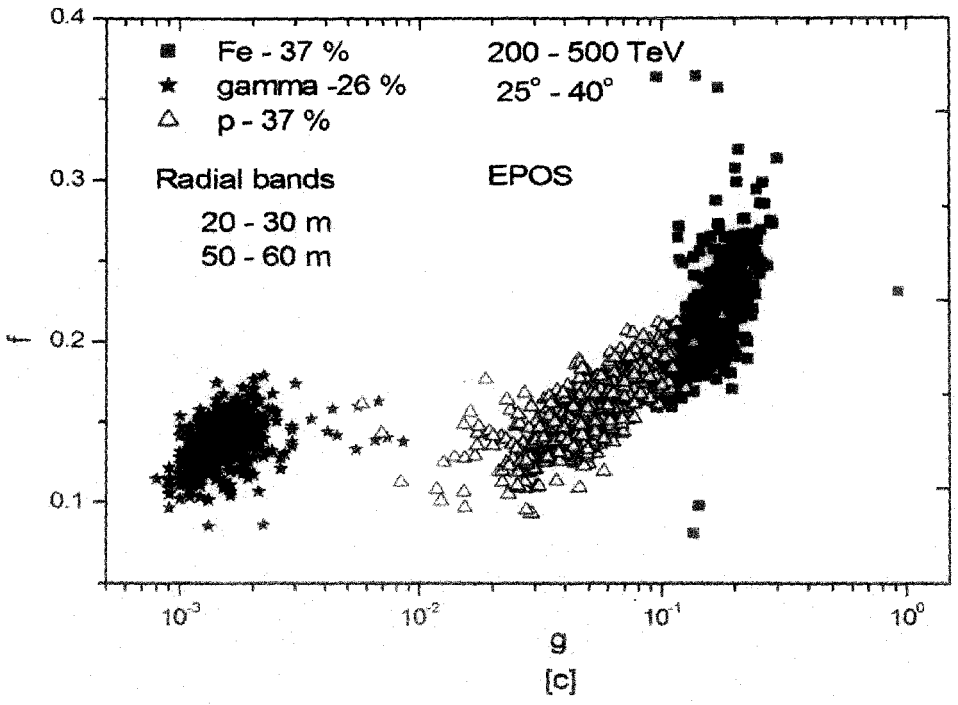

Fig.4.3: Distribution of EAS events generated in the zenith angle interval 25^0 – 45^0 in the $g-f$ plane at ARGO-YBJ level: [a] The ratio (f) for two electron densities are taken between distance bands $5-15$ m and $35-45$ m using the interaction model QGSJet; [b] Same as Fig.4.3a but distance bands are taken at $20-30$ m and $50-60$ m respectively; [c] Same as Fig.4.3b but with the hadronic interaction model EPOS. A negligible percentage of γ-ray primaries are found behind hadron (proton) showers.

4.8 GAMMA-RAY SEPARATION POWER OF METHOD I AND METHOD II

Attempts have been made to discriminate γ-ray showers from hadron initiated showers through method I without taking muon number as an observable. In method I, the r-independent age parameter $s_\perp$ itself is not capable of separating γ-ray showers from the background. This is already revealed in **Fig.4.2a**. The variations of $s_\perp$ and $< s_{local} >$ with N_e in **Fig.4.4a** and **Fig.4.4b** also reaffirm the inability of method **I** over method **II** for the purpose of hadron rejection. From **Fig.4.4a** (also **Fig.4.2a**), it is clear that $s_\perp$values are much nearer to one another corresponding to any N_e-values for both γ-ray and p showers. This ambiguity of method **I** could be well understood if one studies the frequency distribution of $< s_\perp >$ and $< s_{local} >$ for p, Fe and γ-ray showers. Such a study is presented through **Fig.4.4c** and **Fig.4.4d** with the interaction model EPOS at ARGO-YBJ

location. This feature remains unaltered even with the QGSJet model. In **Fig.4.4c**, a major part of the area under the curve of p induced showers is superimposed by the area of γ-ray showers. But from the **Fig.4.4d**, the results seem to be very promising, hinting the possible usefulness of the parameter s_{local} in contrast to $s_{\perp}$ for hadron rejection.

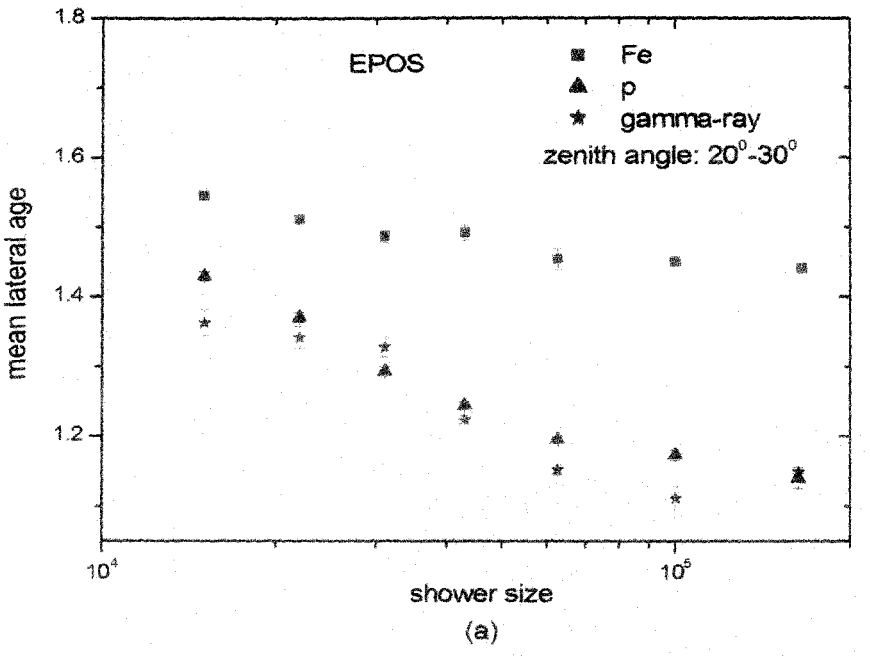

(a)

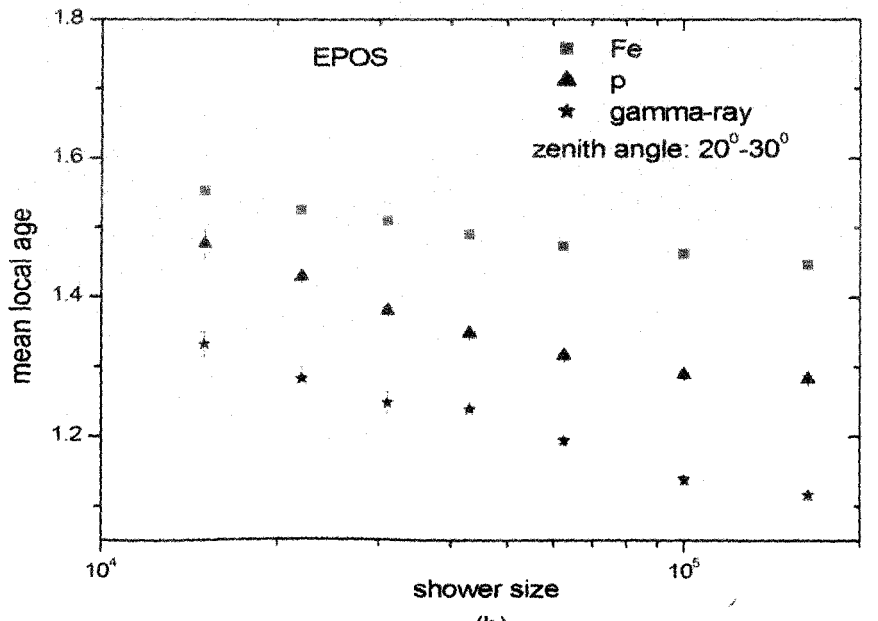

(b)

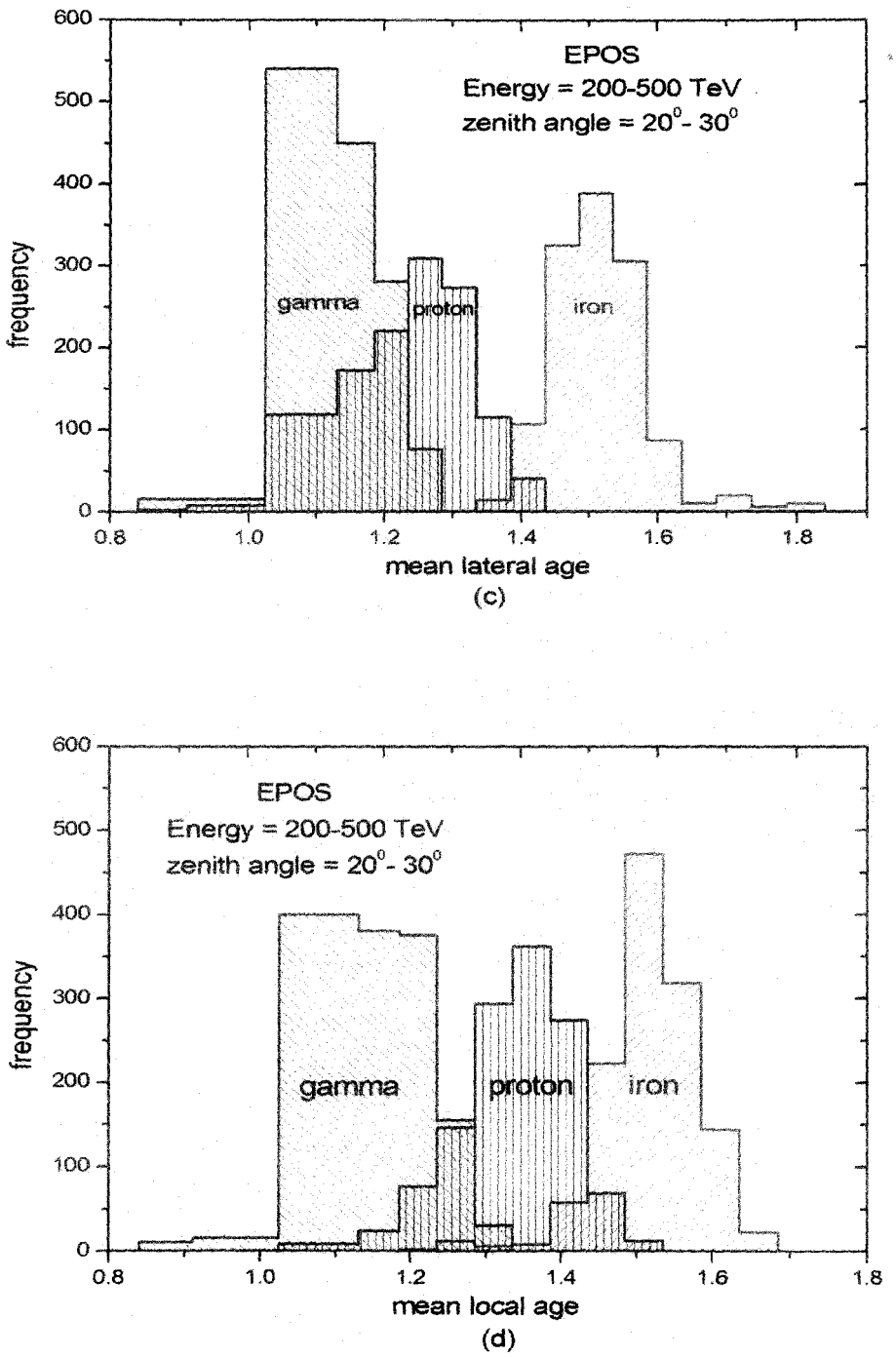

Fig.4.4: [a] Variation of $< s_{\perp} >$ employing method I with N_e at ARGO-YBJ level; [b] Same as Fig.4.4a but with method II; [c] Frequency distribution of $< s_{\perp} >$ and [d] Frequency distribution of $< s_{local} >$.

We would therefore explore through MC simulation study whether LAP is sensitive on primary mass and consequently the possible role that the parameter may play for separating γ-ray showers from a huge background of hadronic showers in primary CRs. One major challenge in this context, however, is the

reliable and unambiguous estimation of the parameter from the experimentally measured electron densities. Since the LAP is found to vary with radial distance, comparison of LAPs obtained by different EAS experimental groups is difficult as the radius of the shower disc differ from experiment to experiment.

4.9 RESULTS ON GAMMA-HADRON SEPARATION: METHOD II

Due to overwhelming background caused by hadron induced EASs, the discrimination of the rare gamma-like events is vital. The background can be rejected by exploiting the LAP between γ-ray-initiated showers and hadron-initiated ones. Here, we noticed that EAS events those are simulated in the same primary energy range initiated by different primaries may produce different N_e. This feature is manifested in the variation of LAP against N_e. The scatter plots of $< s_{local} >$ versus N_e are shown in **Figs. 4.5a**, **4.5b** and **4.5c** respectively where distribution of different primary masses based on s_{local} and N_e data from the mixture-II corresponding to different primary energies and interaction models are presented.

In the primary CR flux, the percentage of γ-ray flux is very small, of the order of 0.001%. To separate such a small fraction of γ-ray component from primary CRs in a real experiment employing method II, it would be nice if we could prepare a mixture with such a small percent of γ-rays and see whether the γ-ray events can be extracted out or not. But due to limited statistics we could not do that. Instead, we made three sub-mixtures of type II maintaining the ratio of primaries as 37% p, 37% Fe and 26% γ-ray for three different combinations of zenith angle, primary energy and shower size ranges. These exercises are worked out for both the high energy interaction models QGSJet and EPOS. From each sub-mixture, we tried to separate γ-ray showers out exploiting s_{local} corresponding to different N_e.

For a small enough cut value of s_{local} we have found poor acceptance for γ-ray induced EAS and very good rejection of background, whereas for a large enough cut value of s_{local} the selection or rejection ability is found to be completely reversed. Cut values of s_{local} lie between the two extremes offered different acceptances and rejections of γ-ray and background respectively. Similarly an appropriate cut on N_e is also needed for the selection/rejection purpose. In astronomical signal selection, optimal cut to selection parameters is

generally set by numerical maximization of the quality factor Q whose formula is already given by the equation **4.4** in the sub-section **4.5.2**.

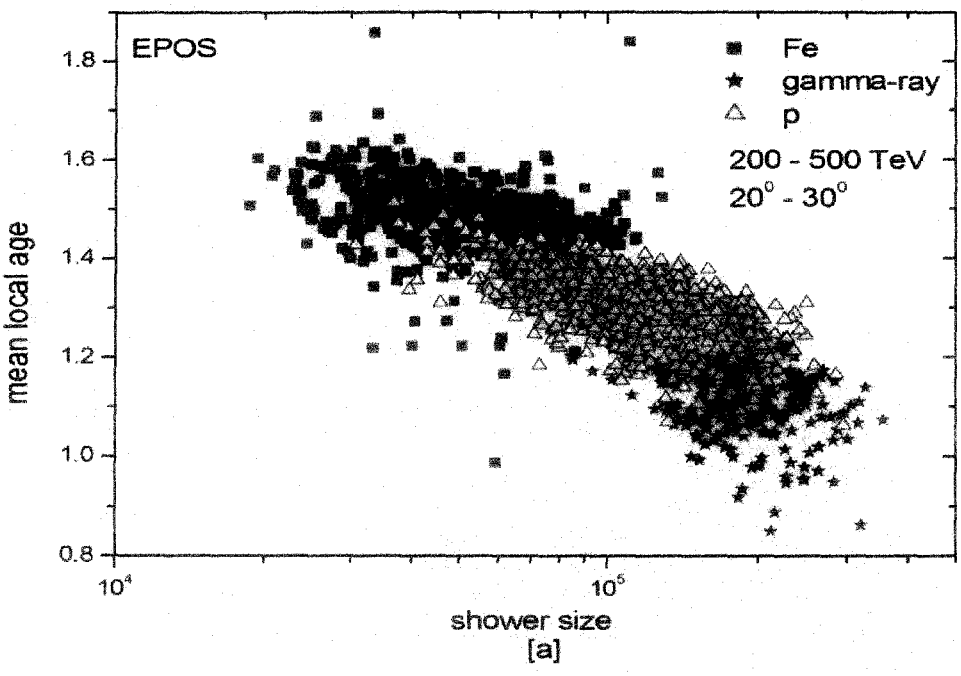

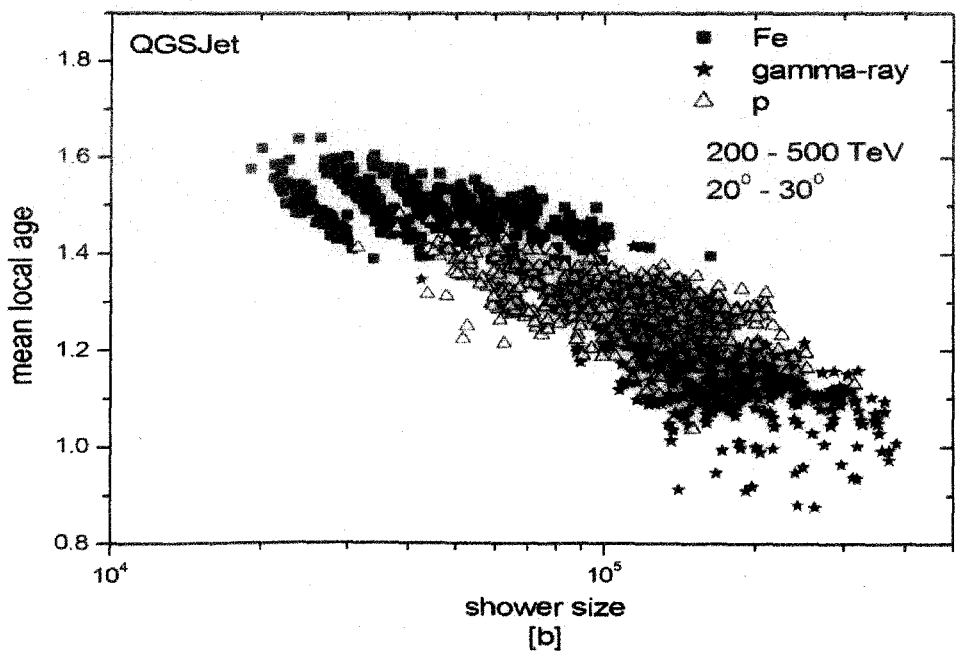

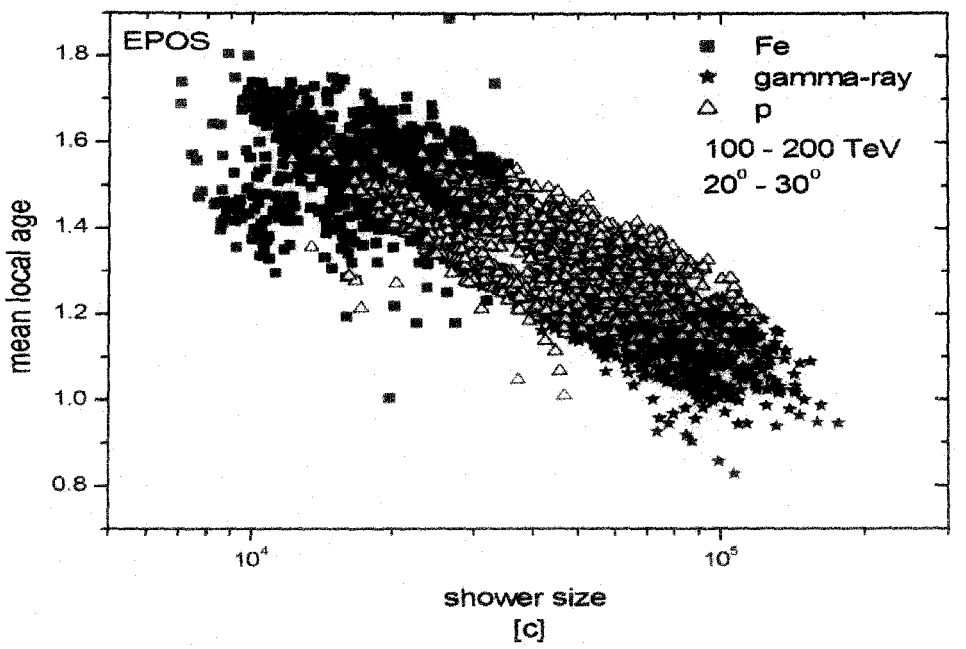

Fig.4.5: [a]-[c] Distribution of simulated showers in mixture II in two primary energy ranges based on s_{local} and N_e at ARGO-YBJ. Dependence on interaction models is also shown through the figures.

The quality factor Q which measures the discrimination power has been estimated as functions of primary energy, zenith angle and shower size, for different cut values of s_{local} utilized to identify γ-ray-initiated air showers against hadron-initiated ones is shown in **table 4.1**. In **table 4.2**, we have given a chart for quality factors estimated at optimal conditions under three different selection criteria.

Another background rejection technique to evaluate the performance of selection algorithm is the application of advanced technique like Principal Component Analysis (PCA) or a Fisher Analysis that allows combining s_{local} and N_e in a single optimized observable.

s_{local}	1.05	1.08	1.10	1.12	1.14	1.15	1.16	1.18	1.20
ϵ_γ	0.146	0.237	0.348	0.510	0.657	0.707	0.778	0.864	0.934
ϵ_{bkg}	0.007	0.022	0.029	0.036	0.058	0.065	0.109	0.145	0.254
Q	1.74	1.61	2.05	2.69	2.73	2.77	2.36	2.27	1.86

Table 4.1: The quality factors at various s_{local} cuts using the interaction model QGSJet. The primary energy, zenith angle and shower size intervals are $200-500$ TeV, $20^0 - 30^0$ and $(1.5-4.0)\times 10^5$ respectively.

Model	E (TeV)	θ (deg.)	$N_e \times 10^5$	s_{local}	ϵ_γ	ϵ_{bkg}	Q
EPOS	100-200	5-15	0.6-2.0	1.14	0.691	0.072	2.57
EPOS	200-500	20-30	1.5-4.0	1.15	0.734	0.048	3.35
QGSJet	200-500	20-30	1.5-4.0	1.15	0.707	0.065	2.77

Table 4.2:The different signal selection parameters at optimal conditions.

4.10 DISCUSSION AND CONCLUSIONS

In this chapter, attempts have been made to discriminate γ-ray induced EAS from hadron initiated shower on the basis of shape of electron density distribution in EAS characterized by lateral shower age parameter that essentially reflects the stage of EAS development in atmosphere. Generally muon content of an EAS is treated as a good estimator for gamma-hadron discrimination. However, a precise measurement of total muons in an EAS requires muon detectors covering large area which is quite expensive. So, we explored whether lateral shower age could be used for the purpose.

We first explored traditional lateral shower age parameter i.e. single (r-independent) shower age as the distinguishing parameter. Later, we attempted to separate out γ-ray initiated EAS on the basis of mean LAP. It is found from the simulation results that γ-ray induced EASs are younger in terms of the mean LAP (i.e. having lower mean LAP) and hence this parameter can effectively separate out γ-ray induced showers from hadronic EAS unlike the case of single lateral shower age. This is probably because of the inadequacy of a single (constant) lateral age parameter to describe the experimental lateral distribution of EAS electrons properly at all distances as noted in several experimental observations. So when a single constant age is assigned (from fitting of the electron density data at different radial distances) to an EAS event, the discriminating power of that parameter on primary masses somewhat becomes dull; it still can distinguish iron initiated showers from proton induced showers but can't effectively separate out γ-ray showers from EASs generated by primary protons. **Fig.4.4a** and **Fig.4.4c** are indicative ones in favour of the inadequacy of $s_{\perp}$ for gamma-hadron discrimination. It is clear from these figures that $< s_{\perp} >$ values for γ-ray and proton induced showers are very much nearer to each other. Lateral distribution of electrons in EAS exhibits universal (primary energy and mass independent) behaviour in terms of LAP (Dey et al. 2012). The present conclusion appears independent on the choice of high energy interaction models, or at least does not have strong interaction model dependence as both the QGSJet and EPOS give similar results.

An important question is the experimental realization of the adopted technique involving LAP. The uncertainty in estimating LAP is usually large in normal circumstance in comparison to that in lateral shower age as the LAP depends on the logarithmic derivative of the electron density versus radial distance. Thus, uncertainty in estimating LAP from experimental data arises mainly from the uncertainties in electron densities and those in radial distance measurements due to erroneous determination of shower core position. These uncertainties should be small for a closely packed air shower array like GRAPES III at Ooty (Gupta et al. 2005) or for a full coverage EAS array like ARGO-YBJ (Sciascio et al. 2007 & Aloisio et al. 2001) and hence the proposed method may successfully work in such kind of experiment. However, at present the ARGO-YBJ carpet provides a full coverage area of about $80m \times 80m$. For successful implementation of the proposed method, a slightly larger coverage area of the carpet would be desirable.

We also tried to identify γ-ray generated EAS by the use of f parameter that describes the ratio of reconstructed average LEDs at two arbitrary distance bands from the shower core as proposed in (Sciascio & Girolamo 2007, Aloisio et al. 2001, Gaisser & Stanev 1991). It is found from the scatter plot of f (as $\boldsymbol{y}$ variable) with the ratio of total muon content to total electron number ($\boldsymbol{x}$ variable) that EAS events are classified according to their respective primaries but the separation occurs not along $\boldsymbol{y}$-axis rather along $\boldsymbol{x}$-axis. This means that essentially the separation is due to the total muon content in EAS, a well studied mass sensitive observable.